



LAWRENCE
LIVERMORE
NATIONAL
LABORATORY

Global and Local Mechanical and Fabric Measurements of Sand Using DEM

P. Fu, Y. F. Dafalias

August 3, 2011

2012 GeoCongress, ASCE
Oakland, CA, United States
March 25, 2012 through March 29, 2012

Disclaimer

This document was prepared as an account of work sponsored by an agency of the United States government. Neither the United States government nor Lawrence Livermore National Security, LLC, nor any of their employees makes any warranty, expressed or implied, or assumes any legal liability or responsibility for the accuracy, completeness, or usefulness of any information, apparatus, product, or process disclosed, or represents that its use would not infringe privately owned rights. Reference herein to any specific commercial product, process, or service by trade name, trademark, manufacturer, or otherwise does not necessarily constitute or imply its endorsement, recommendation, or favoring by the United States government or Lawrence Livermore National Security, LLC. The views and opinions of authors expressed herein do not necessarily state or reflect those of the United States government or Lawrence Livermore National Security, LLC, and shall not be used for advertising or product endorsement purposes.

Global and Local Mechanical-Fabric Measurements in Granular Assemblies Using DEM

Pengcheng Fu¹ and Yannis F. Dafalias^{2,3}

¹Atmospheric, Earth, and Energy Division, Lawrence Livermore National Laboratory, 7000 East Avenue, L-286, Livermore, CA 94550, USA; PH (925) 422-3579; email: fu4@llnl.gov

²Department of Civil and Environmental Engineering, University of California, Davis, CA 95616, USA; jfdafalias@ucdavis.edu

³Department of Mechanics, School of Applied Mathematical and Physical Sciences, National Technical University of Athens, Zographou Campus, Athens

ABSTRACT

Classical soil mechanics treats a soil sample subjected to laboratory testing as a homogeneous soil element and uses the homogenized strains in constitutive modeling. This method does not appropriately consider the fact that strain localization (i.e. shear banding) is almost an inevitable phenomenon in soils. After shear banding takes place, the continued deformation of the sample localizes in one or few shear bands, whereas the remaining portions experience essentially rigid body motions along the shear bands. In this situation, the mechanical interpretation of homogenized (i.e. average) measurements of soil element behaviors becomes ambiguous, and the effort of constitutive modeling should focus on local measurements within the shear bands whenever applicable. The present paper describes a number of innovative local quantification techniques that we have recently developed or tailored on a numerical platform in order to facilitate characterizing soil behaviors within shear bands. With these new techniques, we compare average mechanical and fabric measurements homogenized over the entire sample, to those retrieved from the shear bands only in the context of numerical simulation with the discrete element method (DEM).

INTRODUCTION

Classical soil mechanics has traditionally treated a soil sample subjected to laboratory testing (triaxial, plain strain compression, simple shear, true-triaxial, hollow cylinder, etc.) as a soil element and uses the homogenized strains in constitutive modeling. Although deformation localization, especial shear banding is often observed, it is usually not explicitly considered at the specimen level in most constitutive theories. However, it has been discovered in experimental studies utilizing advanced imaging technologies that strain localization is almost a universal phenomenon for both loose and dense sand specimens under drained as well as undrained test conditions (Finno et al. 1996, 1997). X-ray computed tomography (CT) analysis (Desrues et al. 1996) has revealed that some seemingly uniform deformation patterns are in fact the results of complex shear localization (or shear banding) patterns inside soil specimens. After shear banding takes place, the continued deformation of the sample concentrates in one or a few shear bands, whereas the remaining portions experience essentially rigid body motions along the shear bands. In this situation, the mechanical interpretation of homogenized (i.e. average) measurements of soil element behaviors becomes ambiguous, and the effort

of constitutive modeling should focus on measurements local to the shear bands. Despite the significant advance in laboratory measurement technologies (e.g. Desrues and Viggiani, 2004; Rechenmacher, 2006; Hall et al., 2010; Hasan and Alshibli, 2010), local quantification of shear band characteristics remains an expensive and technically challenging task that is not available to most laboratories. Note that shear failure planes in the field can be seen as a form of shear bands. This situation is typically handled explicitly in numerical models by allowing state variables for the failed elements to evolve differently from those for the remainder of the geo-structure. This paper focuses on the interpretation of laboratory test results and its implications for constitutive modeling.

Particle-based numerical methods, especially the discrete element method (DEM, also termed the distinct element method) provide an appealing supplement to laboratory experiment. DEM simulation yields a complete time history of information about velocity and location of all the particles constituting the assembly being simulated as well as their mutual relationships (i.e. contacts and contact forces). This makes the comparison of material characteristics quantified locally and globally a reasonably achievable task. Unfortunately, most studies in the literature employing DEM simulation have followed the tradition of global measurements as in laboratory studies. This is partly due to the lack of analysis methods designed for local quantities, so the analysis of DEM simulation results largely continues to use analysis methods analogous to laboratory measurements.

In this paper, we present some of the advances that we have made in using DEM to investigate granular material properties, especially those local to shear bands. We first present the analysis methods developed and tailored for this purpose. Then we compare the local and global analysis results to gain insights into the implications of local measurements for the study of soil mechanics. As mentioned before, we see DEM numerical simulation as a promising supplement (not a replacement) for traditional laboratory methods. Although DEM is not capable of capture all the features of real soil samples, the insights that we gained in the numerical platform could inspire and guide the study of real materials.

LOCAL MEASUREMENT TECHNIQUES

Identification of Shear Bands and Masking

Shear bands in laboratory experiments are usually identified in a subjective way through the discontinuous deformation patterns. DEM simulation provides abundant information about the movement of individual particles, allowing more objective methods of shear localization identification. Shown in Figure 1 are the DEM simulation results of a biaxial compressive test under constant lateral confining stress at an axial strain of 15%. Figure 1(a) shows the deformed grid “painted” onto the specimen in its undeformed state; in Figure 1(b) the color of each particle denotes the amount of rotation since the initial state; the line segments in Figure 1(c) represent the maximum shear strain rate, with the lengths denoting magnitudes and the orientations denoting the maximum shear direction. These three methods unanimously show a shear band extending diagonally in the specimen. Once a shear band is identified, we can attach a polygon-shaped “mask” covering the center

portion of the shear band. Each vertex of this mask is attached to a particle so that the mask can deform with the sample as shown in Figure 1(a). Most mechanical characteristics of a granular particle assembly modeled with DEM, including stress, strain and strain rates, void ratio, fabric tensor, etc. are obtained through statistical analysis of particle-level quantities. By only including quantities pertaining to particles or inter-particle contacts within the mask, we can obtain quantitative characteristics of the shear band.

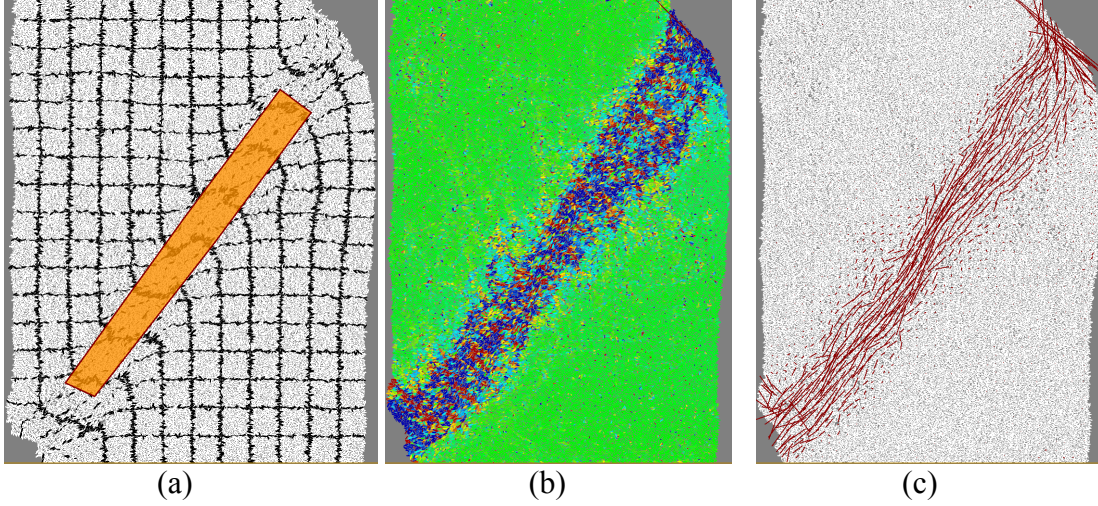


Figure 1 Various methods for identifying shear bands. Details of the simulations have been reported in Fu and Dafalias (2011a, b) and are not repeated here. A mask covers the center portion of the shear band and deforms with the specimen in shown in (a).

Quantifying Local Deformation

We have also developed a method for quantifying large and localized deformation in granular assemblies. Existing methods typically discretize the equivalent continuum of granular assembly into a mesh and use formulations analogous to the strain calculation methods in the finite element method (FEM) to quantify the deformation of this granular assembly. The new method presented here is based on the velocity gradient tensor instead of small engineering strains. We rely on “reference triangles” to estimate the velocity gradient of arbitrary domains composed of multiple particles in the assembly. A reference triangle for a small domain in a granular assembly is shown in Figure 2. Its three vertices are attached to three particles with coordinates \mathbf{x}^1 , \mathbf{x}^2 , and \mathbf{x}^3 and velocity \mathbf{v}^1 , \mathbf{v}^2 , and \mathbf{v}^3 . The four components of the velocity gradient tensor \mathbf{L} ($v_{i,j}$) are

$$\begin{bmatrix} v_{1,1} \\ v_{1,2} \\ v_{2,1} \\ v_{2,2} \end{bmatrix} = \frac{1}{2A} \begin{bmatrix} x_2^2 - x_2^3 & 0 & x_2^3 - x_2^1 & 0 & x_2^1 - x_2^2 & 0 \\ x_1^3 - x_1^2 & 0 & x_1^1 - x_1^3 & 0 & x_1^2 - x_1^1 & 0 \\ 0 & x_2^2 - x_2^3 & 0 & x_2^3 - x_2^1 & 0 & x_2^1 - x_2^2 \\ 0 & x_1^3 - x_1^2 & 0 & x_1^1 - x_1^3 & 0 & x_1^2 - x_1^1 \end{bmatrix} \begin{bmatrix} v_1^1 & v_2^1 & v_1^2 & v_2^2 & v_1^3 & v_2^3 \end{bmatrix}^T \quad (1)$$

According to definitions in continuum mechanics, the rate-of-deformation tensor \mathbf{D} and the spin tensor \mathbf{W} are the symmetric and skew-symmetric parts of tensor \mathbf{L} , respectively. Multiple reference triangles can be defined for the same domain and since they are independent of each other, they can geometrically overlap. The sizes of

the reference triangles can be selected according to the resolution requirement of the analysis. Because only the locations and velocities of the current time step is used and a “reference configuration” is not required to define the velocity gradient, the reference triangles at different times steps do not necessarily attach to the same particles. For the purpose of quantifying deformation (rates) in a shear band, the reference triangles should be smaller than the width of the shear band. Numerous overlapping reference triangles can be created to cover the entire specimen, but statistical analysis can be conducted only on the ones within the shear band mask.

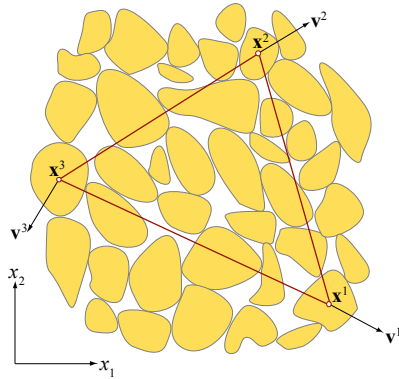


Figure 2 A reference triangle for a small domain in a granular assembly.

The aforementioned tensors (**L**, **D**, and **W**) only provides information about the “rate” of deformation at any given moment. In order to track the overall shear deformation of a shear band, we can perform a time integration of the shear component of **D** along the shear band direction. The integral is termed the accumulative local shear strain in the following numerical examples.

Quantifying Local Void Ratio

The void ratio of an identified shear band can be calculated based on the total area (the 2D equivalent of volume) of the masked shear band and the volume of the solid phase inside. However, this is a nontrivial task because many particles are arbitrarily “split” by the edges of the mask into two halves, one inside the mask and the other outside. To avoid the complexity caused by the calculation of the areas of these two arbitrary halves, we rasterize the DEM model into a high-resolution bitmap image. Each particle is typically represented by thousands to tens of thousand pixels in the bitmap, depending on the particle size. The void ratio in the masked shear band is calculated by dividing the number of pixels representing voids by the number of pixels representing solid particles in the mask. Checking whether a given pixel is inside the polygon-shaped mask is a trivial task.

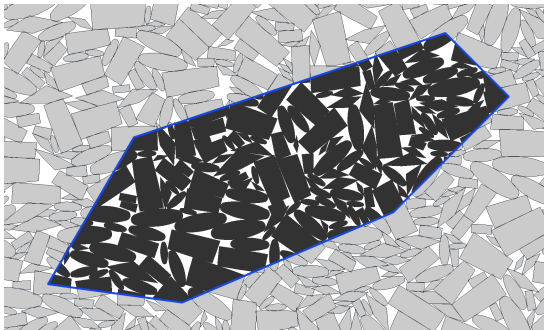


Figure 3 Rasterizing the DEM model into a bitmap for calculating the void ratio in the mask. Solid particles in the mask are represented by black pixels and voids represented by white pixels. Note that this arbitrary mask is for illustrative purposes, and it does not necessarily cover a shear band in this specific image.

NUMERICAL EXAMPLE I: SIZE-EFFECT ON VOLUMETRIC STRAIN

In soil mechanics, the volumetric strain ε_v of a particle assembly (or a soil sample) is calculated as

$$\varepsilon_v(t) = \frac{V(t) - V_0}{V_0} \times 100\% \quad (2)$$

where V_0 is the total volume of the undeformed specimen (the reference configuration) and $V(t)$ is the specimen volume at time t . The average void ratio can be calculated based on the volumetric strain as

$$\bar{e}(t) = (1 + e_0) (1 + \varepsilon_v) - 1 \quad (3)$$

If we explicitly take the effects of shear banding into account, we can assume that: 1) in the undeformed homogeneous state, the volume ratio of the portion that would evolve into shear bands to the entire specimen is α ; 2) the average void ratio of the shear band(s) is $e_s(t)$, and 3) the void ratio of the remainder of the specimen is $e_r(t)$. The average void ratio over the specimen is then

$$\bar{e}(t) = \alpha e_s(t) + (1 - \alpha) e_r(t) \quad (4)$$

and $e_s(t)$ and $e_r(t)$ are dependent on the stress state at time t as well as some intrinsic properties of the particle assembly itself. Therefore, the average void ratio calculated based on the overall deformation of the specimen is actually dependent on a geometrical parameter α . It has been observed in the literature that the width of a shear band is typically 8 to 20 times the mean particle size (Muhlhaus and Vardoulakis, 1987; Finno et al., 1997; Alshibli and Sture, 1999), so the value of α is likely to decrease as the specimen size increases. Due to this mechanism, the volumetric strain, as well as the corresponding void ratio at a given stress state and total deformation level is dependent on the sizes of the specimen.

This size effect was not paid attention to in soil mechanics probably because each laboratory usually employs soil samples of the same size. While it is uncommon to test otherwise identical soil samples with different sizes in a real laboratories, DEM provides a convenient means for demonstrating this phenomenon. In the following example, a biaxial compression specimen (denoted as specimen A) with a height-to-width ratio of approximately 2.2 is fabricated with the pluviation method described in Fu and Dafalias (2011a). This specimen consists of 18,000 pentagonal particles of various sizes. Two more specimens (B and C) are trimmed out of specimen A, and they consist of 9,000 and 4,500 particles, respectively but the height-to-width ratios remains 2.2. All three specimens are subjected to isotropic consolidation at a confining pressure of 100 kPa and the initial average void ratio is 0.173. Subsequently, they are axially compressed at the same strain rate while the confining pressure (σ_3) remains at 100 kPa. The deformation patterns of the three specimens are shown in Figure 4. Two shear bands forming an “X”-shaped pattern have developed in each specimen. This is in part because the upper and lower platens compressing the specimens are not allowed to move laterally, forcing such an “X”-shaped pattern to form.

If we were to investigate the global behavior of these three specimens, the evolution of the stress ratio σ_1/σ_3 and the volumetric strain is show in Figure 5. Typical behaviors of dense sand can be observed. The stress ratio for all the three

specimens first reaches a peak value before declining to a constant value (the so-called steady or critical state) with minor fluctuation. The three specimens share the same peak stress ratio and the same critical stress ratio, as expected. In terms of the volume change, significant dilation is observed after a brief volume decrease, typical of dense sands. All three specimens eventually reach constant volumetric strains, but the steady-state volumetric strain increases as the size of the specimen decreases. This can be explained by equation (4) as the average void ratio as well as the corresponding average volumetric strain increases as α , the relative volume of the shear band compared to the volume of the specimen increases. Since the width of the shear band is closely related to the particle sizes, it does not change proportionally as the specimen is composed of less or more particles. We can also observe that the three axial strain-volumetric strain curves only “split” from each other at an axial strain of approximately 4%, when shear banding starts to dictate deformation of these specimens. Before that they exactly overlap each other.

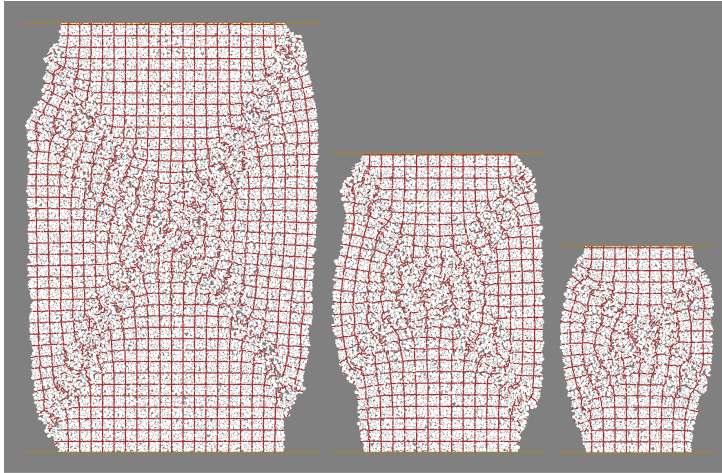


Figure 4 Shear banding patterns of the three specimens with the same initial state but different sizes: They consist of 18,000, 9,000, and 4,500 particles from left to right. At the same overall axial deformation, shear bands in a smaller specimen occupy a larger portion of the total volume.

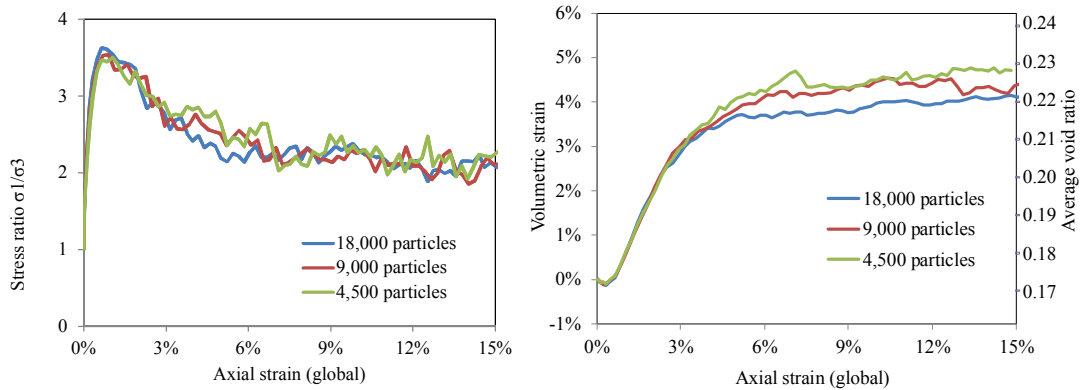


Figure 5 Global responses of the three biaxial compression specimens.

This dependency of the critical (or steady) state void ratio on the specimen sizes is troublesome in constitutive modeling. Material characteristics in the critical state are supposed to be inherent material properties, and parameters related to specimen dimensions are highly undesirable in constitutive models. A solution is to focus the measurement in the shear bands, where deformation is actually taking place, instead of the specimen as the whole. Figure 6 shows the evolution of void ratios of

the three specimens in the shear bands with respect to the local accumulative shear strain. They all converge to the same local void ratio of 0.30. The random fluctuation of the local void ratio is more severe than that of the global measurement, because the shear bands only comprise a relatively small number of particles. Since real specimens are usually made up of millions to billions of particles, this volatility should not be a serious issue for real specimens.

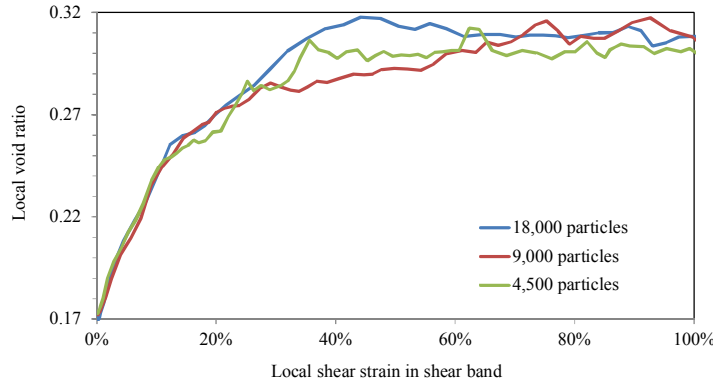


Figure 6 The evolution of void ratio inside shear bands with respect to the local accumulative shear strain of the shear bands.

EXAMPLE II: BIAXIAL COMPRESSION WITH DIFFERENT INITIAL PARTICLE ORIENTATION

Strength and deformation characteristics of sands with inherent fabric anisotropy caused by preferred alignment of elongated particles perpendicular to the direction of deposition have been extensively studied both experimentally (e.g. Oda et al., 1978; Tatsuoka et al., 1986; Guo, 2008) and numerically (e.g. Mahmood and Iwashita, 2009; Li and Li, 2009; Fu and Dafalias, 2011a and 2011b). Figure 7 shows selected results from a numerical investigation using DEM (Fu and Dafalias, 2011a). The discrete model used in the study, the fabrication of the numerical specimens, and the simulation parameters were reported in Fu and Dafalias (2011a, 2011b) and Fu et al. (2011). The results shown here are the evolution of the principal stress ratio and volumetric strain of biaxial compression tests with different initial predominant particle orientations (characterized by the bedding plane tilting angle δ) but otherwise the same initial fabric (void ratio, intensity of fabric anisotropy, etc.). These numerical results quantitatively resemble the plane strain compressive test results on natural sands reported by Oda et al. (1978) and Tatsuoka et al. (1986). According to these global average measurements, the steady-state volumetric strain (and critical void ratio) seems to depend on the initial particle orientations with respect to the loading directions. The specimens with its bedding plane perpendicular or approximately perpendicular to the major principal stress ($\delta=0^\circ, 15^\circ$) have the greatest dilation rates and ultimate volumetric strains. This observation has influenced subsequent modeling efforts (e.g. Dafalias et al., 2004), which formulated the steady-state void ratio as a function of the initial fabric.

However, if we focus the measurement on the shear band only, as shown in Figure 8, we can observe that local void ratio in all specimens tends to approach the same ultimate value of approximately 0.30. Note that the seven curves terminate at different local shear strains (from 120% for $\delta=60^\circ$ to 370% for $\delta=0^\circ$), but the ends correspond to the same global axial strain of 24%. As shown in Figures 9, the

relationship between the global axial strain and the local shear strain in shear bands is complicated. Some specimens, such as that with $\delta=0^\circ$ develop thin shear bands at an early stage of deformation. The shear bands in some other specimens such as those with $\delta=60^\circ$ or $\delta=90^\circ$ are rather dispersed. At the same axial strain, the shear band deformation rate for the former is higher than that for the later, allowing various amounts of accumulative deformation to develop in the shear bands. For the latter specimens, the total shear deformation in shear bands does not seem to be sufficient to allow the ultimate void ratio to be reached when the loading has terminated. Although the ultimate fabric characteristics at very large deformation seem to be independent of the initial fabrics, the fabric evolution processes do depend on the initial fabrics.

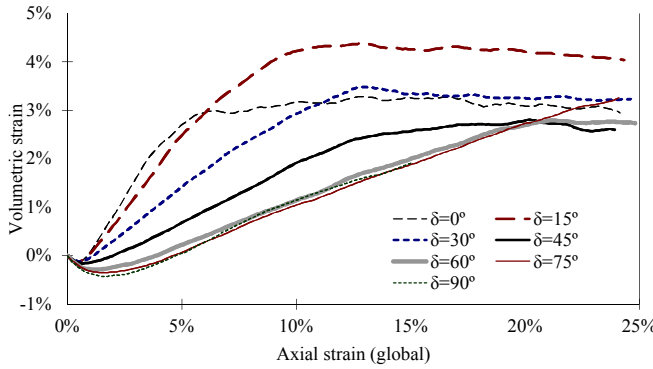


Figure 7 The evolution of volumetric strain in biaxial compression test simulations with different initial particle orientations. The tilting angle δ is the angle between the bedding plane of particle pluviation and the plane of major principal stress. (This is a modified version of Figure 9 in Fu and Dafalias, 2011a)

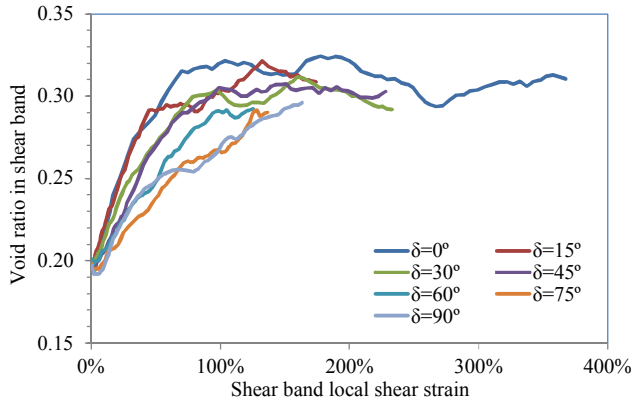


Figure 8 The evolution of shear band local void ratio with respect to the local accumulative shear strain in shear bands.

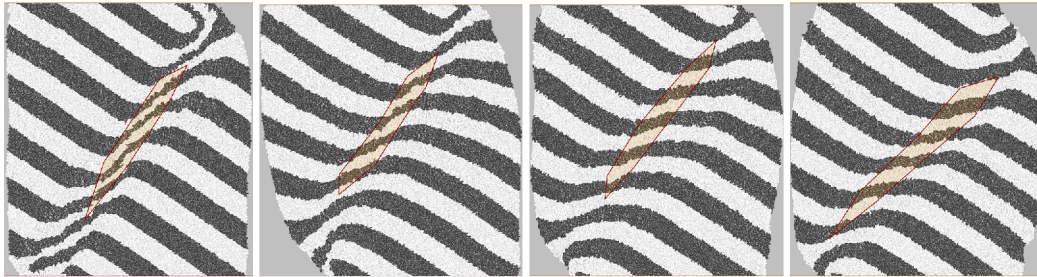


Figure 9 Deformation pattern of selected specimens in the end of loading (global axial strain of 24%). The polygon-shaped semi-transparent areas are the masks used for local measurement. They only cover the center portion of the shear bands, not necessarily the full width.

CONCLUDING REMARKS

The present paper discusses the implications of global (covering the entire laboratory test or numerical specimens) vs. local (focusing on the shear bands only) measurements for constitutive modeling of soils. The former has been the mainstream methodology, largely owing to the fact that quantification of soil characteristics local to shear bands is inevitably difficult in a laboratory environment. Particle-based numerical methods, such as the discrete element method (DEM) provide a promising research platform where local measurement can be conducted in a relatively easy manner. However, due to the long tradition of global quantification, methods and numerical tools for local measurement are far from being widely available. We have been trying to revisit some important problems in soil mechanics with innovative local measurement techniques on a DEM-based numerical platform. This paper presents some of the methods and numerical tools that we have developed, and also illustrates the importance of local measurements by comparing the conclusions that would be drawn from traditional global measurements and the observations made with the relatively new local quantifications. It was found that focusing the deformation in shear bands reveals some “simple and clear” soil behaviors, which are desirable in constitutive modeling. The preliminary observations suggest that certain behaviors such as the dependency of the steady-state (or critical-state) void ratio on specimen sizes or initial predominant particles orientations can be artifacts introduced by averaging soil characteristics across the entire specimens. Nevertheless, to build new constitutive models based on local measurements is a challenging task. Rather than presenting a mature solution, the present paper only aims at introducing our preliminary effort that can potentially be useful to ongoing studies in this area.

ACKNOWLEDGMENTS

Pengcheng Fu’s work in this paper was partly performed under the auspices of the U.S. Department of Energy by Lawrence Livermore National Laboratory under Contract DE-AC52-07NA27344. This document has been released by LLNL to the public (LLNL-CONF-491802). The research leading to these results has received funding from the European Research Council under the European Union's Seventh Framework Program (FP7/2007-2013, IDEAS) / ERC grant agreement # 290963, with acronym SOMEF and Yannis F. Dafalias the Principal Investigator.

REFERENCES

- Alshibli, K.A., and Sture, S. (1999). “Sand shear band thickness measurements by digital image technique.” *Journal of Computing in Civil Engineering*, 12(2): 103-109.
- Dafalias, Y.F., Papadimitriou, A.G., and Li, X.S. (2004). “Sand plasticity model accounting for inherent fabric anisotropy.” *Journal of Engineering Mechanics*, 130(11): 1319-1333.
- Desrues, J., Chambon, R., Mokni, M., and Mazerolle, F. (1996). “Void ratio evolution inside shear bands in triaxial sand specimens studied by computed tomography.” *Géotechnique*, 46(3): 529-546.
- Desrues, J., and Viggiani, G. (2004). “Strain localization in sand: an overview of the experimental results obtained in Grenoble using stereophotogrammetry.”

- International Journal for Numerical and Analytical Methods in Geomechanics*, 28(4): 279-321.
- Finno, R.J., Harris, W.W., Mooney, M.A., and Viggiani, G. (1996). "Strain localization and undrained steady state of sand." *J. Geotech. Eng.* 12(6): 462-473.
- Finno, R.J., Harris, W.W., Mooney, M.A., and Viggiani, G. (1997). "Shear bands in plane strain compression of loose sand." *Géotechnique*, 47(1): 149-165.
- Fu, P., and Dafalias, Y.F. (2011a). "Study of anisotropic shear strength of granular materials using DEM simulation." *Int. J. Numer. Anal. Methods Geomech.*, 35(10): 1098-1126.
- Fu, P., and Dafalias, Y.F. (2011b). "Fabric evolution within shear bands of granular materials and its relation to critical state theory." *Int. J. Numer. Anal. Methods Geomech.* doi: 10.1002/nag.988.
- Fu, P., Walton, O.R., and Harvey, J.T. (2011). "Polyarc discrete element for efficiently simulating arbitrarily shaped 2D particles." *Int. J. Numer. Meth. Eng.*, doi: 10.1002/nme.3254.
- Guo, P.J. (2008). "Modified direct shear test for anisotropic strength of sand." *J. of Geotech. and Geoenviron. Engineering*, 134(9): 1311-1318.
- Hall, S.A., Bornert, M., Desrues, J., Pannier, Y., Lenoir, N., Viggiani, G., and Béuelle, P. (2010). "Discrete and continuum analysis of localised deformation in sand using X-ray μ CT and volumetric digital image correlation." *Géotechnique*, 60(5): 315-322.
- Hasan, A., and Alshibli, K.A. (2010). "Experimental assessment of 3D particle-to-particle interaction within sheared sand using synchrotron microtomography." *Géotechnique*, 60(5): 369-379.
- Lade, P.V., Nam, J., Hong, W.P. (2008). "Shear banding and cross-anisotropic behavior observed in laboratory sand tests with stress rotation." *Canadian Geotechnical Journal*, 45(1): 74-84.
- Li, X., Yu, H., and Li, X. (2009). "Macro–micro relations in granular mechanics." *International Journal of Solids and Structures*, 46(25-26):4331-4341.
- Mahmood, Z., and Iwashita, K. (2009). "Influence of inherent anisotropy on mechanical behavior of granular materials based on DEM simulations." *International Journal for Numerical and Analytical Methods in Geomechanics*, 34(8): 795-819.
- Mühlhaus, H.B., and Vardoulakis, I. (1987). "The thickness of shear bands in granular materials." *Géotechnique*, 37(3): 271-283.
- Oda, M., Koishikawa, I., Higuchi, T. (1978). "Experimental study of anisotropic shear strength of sand by plane strain test." *Soils and Foundations*, 18(1): 25-38.
- Rechenmacher, A.L. (2006). "Grain-scale processes governing shear band initiation and evolution in sands." *Journal of the Mechanics and Physics of Solids*, 54(1): 22-45.
- Tatsuoka, F., Sakamoto, M., Kawamura, T., and Fukushima, S. (1986). "Shear and deformation characteristics of sand in plane strain compression at extremely low pressure." *Soils and Foundations*, 26(1): 65-84.